A study on microstructural changes of reactor pressure vessel steel after proton irradiation

Hyung-Ha Jin*, Eunsol Ko, Sangyeob Lim, Min-Chul Kim, Junhyun Kwon
Nuclear Materials Safety Research, Korea Atomic Energy Research Institute.
Daedoek-daero 989-111, Yuseoung-gu, Daejeon.
**Corresponding author: hhajin2@kaeri.re.kr*

1. Introduction

Radiation hardening (RH) or embrittlement (RE) of reactor pressure vessel (RPV) under high neutron irradiation exposure is considered as one of detrimental degradations against integrity of pressurized water reactor (PWR) for the long term operation [1]. It has been known that significant development of solute clusters and dislocation loops by neutron irradiation lead to radiation hardening and embrittlement of RPV steel. Several researches on microstructural changes by neutron irradiation have been progressed for the estimation of radiation hardening and embrittlement in highly irradiated RPV steels [2-4]. The in-depth analysis on radiation induced microstructural change of RPV steels is still in progress using advanced microstructural characterization techniques such as analytical TEM and 3D-APT. In this work, a proton irradiation technique has been used for emulating of the neutron irradiation effect in RPV steels. The main objective in this work is to analyze microstructural changes of the proton irradiated RPV steels under high irradiation condition with analytical TEM.

2. Experimental

2.1 Materials

The composition of the experimental steel is given in Table 1. Before the proton irradiation, electro-chemical surface treatment was conducted for damage-free surface.

Table 1 Chemical compositions of the test alloy (wt%)

C	Mn	Ni	Si	Cr	Mo	Cu	Fe
0.19	1.42	0.86	0.04	0.14	0.51	-	Bal.

2.2 Proton irradiation

Proton irradiations were conducted at the Michigan Ion beam Laboratory in the University of Michigan. The General Ionex Tandetron accelerator was used for the proton irradiation experiments. The energy of proton used for the irradiation was 2 MeV. The proton irradiation were conducted at a temperature of 300 ± 5 °C. In this work, one irradiated sample (0.4 dpa) was used for the TEM analysis. The calculated radiation damage (dpa) is shown in Fig. 1. The calculation was performed with full cascade mode in the SRIM code [5]. In the calculation, the displacement energy was set to be 40 eV [6]. According to Fig. 1 of SRIM calculation result, the radiation damage remained constant up to around 15 μm in depth. There was a steep rise at 18 ~ 20 μm in depth.

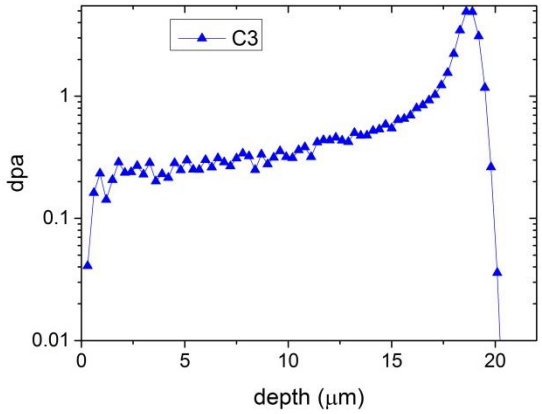

Fig. 1 Radiation damage profiles by calculation of SRIM code

2.3. The preparation of TEM sample

TEM samples were extracted at a depth of ~ 10 μm from sample surface. Electron transparent areas in the TEM samples were obtained using a Tenupol-5 equipment with 7 % perchloric acid in methanol at -40 °C. TEM analysis was conducted for the analysis of typical microstructural changes such as the formation of radiation induced segregation at grain boundary and the formation of radiation defects. Grain boundary composition profiles were measured via scanning transmission electron microscopy (STEM) using the JEM 2100F at Korea Atomic Energy Research Institute, which is equipped with energy dispersive X-ray spectroscopy (EDS).

3. Result and discussion

3.1 Radiation induced segregation at grain boundary

The change of microchemistry at grain boundary was measured by STEM-EDS. The enrichment of Mn and Ni was clearly detected at the grain boundaries as shown in Fig. 2. Radiation induced segregation behavior was also observed at the fine cluster in Fig. 2. Both the grain boundary and cluster were enriched in Ni to levels of 2-3 wt%.

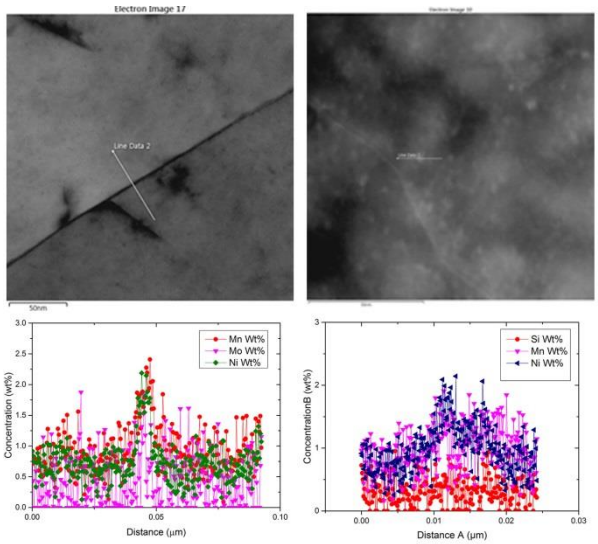

Fig. 2 Concentration profiles at a grain boundary (left) and a fine cluster (right)

3.2. Radiation defects

In the proton irradiated RPV steel, radiation defects are observed in the matrix as shown in Fig. 3. They were seen as black dots in the TEM images. It is difficult to identify the nature of the radiation defects. The spatial distribution of radiation defects was found to be inhomogeneous. Pronounced decoration near dislocations and carbides was observed. No cavity was observed through the TEM analysis.

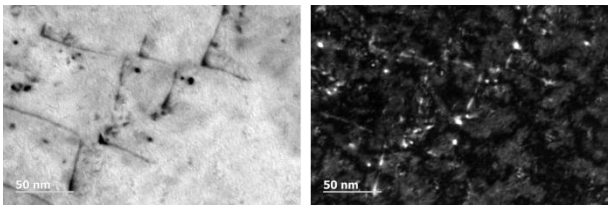

Fig. 3 Bright field TEM image (left) and dark field TEM image (right) showing black dots in matrix which developed after proton irradiation.

3.3. Microstructural Change of Carbide after proton irradiation

TEM observation in Fig. 4 shows instability of pre-existing carbides after proton irradiation. Different contrasts are clearly observed at the interface of carbide in the Fig. 4. TEM-EDS analysis across the carbide (Mo rich carbide, Mo_2C) revealed that the Mo profile shows a local drop in the interface of the carbide. The analysis lead to a finding that the contrast change in the carbide is expected to be caused by dissolution of carbide forming elements such as Mo and Mn.

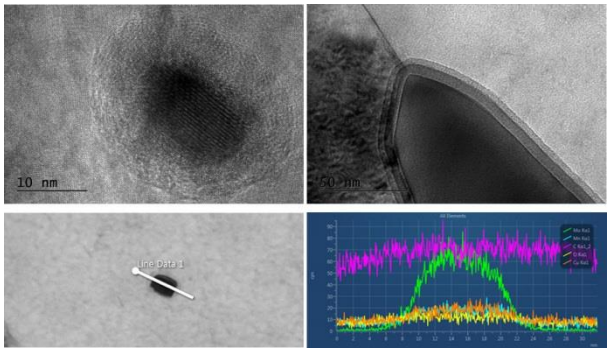

Fig. 4 Changes of morphology of carbides after proton (above) and EDS analysis result across the Mo_2C carbide (below)

4. Conclusions

Microstructural changes of RPV steel after high proton irradiation were investigated with analytical TEM characterization techniques.

(1) The RIS behavior of Mn and Ni was detected at grain boundaries and clusters.
(2) Radiation defects visible in TEM were developed heterogeneously in vicinity of dislocations and pre-existing carbides.
(3) The dissolution of carbide forming elements in carbide will provide another clue for revealing of acceleration of radiation embrittlement in RPV steels since the nature of carbides in RPV steels is known to play key role in the fracture strength changes.

REFERENCES

[1] G.R. Odette, R.K. Nanstad, Predictive reactor pressure vessel steel irradiation embrittlement models : Issues and opportunities, JOM, 61 (7) pp.17-23, 2009.
[2] P B. Wells, T. Yamamoto, B. Miller, T. Milot, J. Cole,Y Wu, G. R. Odette, Evolution of manganese–nickel–silicon-dominated phases in highly irradiated reactor pressure vessel steels, Acta Materialia, 80 pp. 205-219, 2014.
[3] F. Bergner, F. Gillemot, M. Hernández-Mayoral, M. Serrano, G. Török, A. Ulbricht, E. Altstadt, Journal of nuclear materials, 461 pp. 37-44, 2015.
[4] P.D. Styman, J.M. Hyde, K. Wilford, A. Morley, G.D.W. Smith, Precipitation in long term thermally aged high copper, high nickel model RPV steel welds, Progress in Nuclear Energy, 57 pp. 86-92, 2012.
[5]J.F.Ziegler, J.P.Biersack, U.Littmark, The Stopping and Range of Ions in Solids, Pergamon Press, New York, 1985.
[6]ASTM Standard E693-01, Standard practice for characterizing neutron exposure in iron and low alloy steels in terms of displacements per atom (dpa), 2001.
of Nuclear Materials, 317, pp. 32- 45,2003.